JOURNAL OF AGRICULTURAL AND FOOD CHEMISTRY

Article

pubs.acs.org/JAFC

Effect of Simultaneous Inhibition of Starch Branching Enzymes I and IIb on the Crystalline Structure of Rice Starches with Different Amylose Contents

Jianmin Man,[†] Yang Yang,[†] Jun Huang,[†] Changquan Zhang,[†] Yifang Chen,[‡] Youping Wang,[†] Minghong Gu,[†] Qiaoquan Liu,[†] and Cunxu Wei*,[†]

[†]Key Laboratories of Crop Genetics and Physiology of the Jiangsu Province and Plant Functional Genomics of the Ministry of Education, Yangzhou University, Yangzhou 225009, China

[‡]Testing Center, Yangzhou University, Yangzhou 225009, China

ABSTRACT: Mutating or inhibiting genes encoding starch branching enzymes (SBEs) can increase the amylose content (AC) of cereals. We analyzed endosperm starches from three rice cultivars with different ACs and from transgenic lines derived from them. The transgenic lines had simultaneously inhibited *SBE I* and *IIb* genes. Compared with the starch from their wild-type parents, the starch from transgenic lines showed significantly increased apparent ACs and lamella size and decreased relative crystallinity, double helix content, and lamellar peak scattering intensity, and altered short-range ordered structure in the external region. These changes were more prominent in the line derived from the high-AC cultivar than in those derived from waxy and low-AC cultivars. Inhibiting both *SBE I* and *IIb* changed the crystalline structure of starch from A-type to C_A-type in lines derived from waxy and low-AC cultivars, and from A-type to C-type in that derived from the high-AC cultivar.

KEYWORDS: *rice, starch branching enzyme, endosperm starch, crystalline structure, C-type crystallinity*

INTRODUCTION

Starch consists of two main components, linear amylose and highly branched amylopectin, and is stored as discrete granules with alternating semicrystalline and amorphous growth rings. The semicrystalline ring is formed by the lamellar structure of alternating crystalline and amorphous regions.[1] The semicrystalline structure of native starch has been well-studied, and its polymorphisms have been revealed by X-ray powder diffraction (XRD) analyses. Typically, there are three types of starch crystallinity, known as A-, B-, and C-types.[2,3] The A-type starch is present in cereal endosperm, and its crystalline structure is formed by amylopectin with short lateral chains and closed branching points. The crystalline structure of B-type starch, contrary to that of A-type, is usually formed by amylopectin with long side chains and distant branching points. B-type starch is found in tuber crops such as potato.[2,3] The C-type starch is a mixture of both A- and B-type allomorphs, rather than a third distinct type of the double helical arrangement. It is usually present in legumes and rhizomes, and it is characterized by central B-type and peripheral A-type allomorphs in its granules.[4,5]

In general, waxy and normal cereal starches show A-type crystallinity, and high-amylose cereal starches show B-type crystallinity.[2,3] For example, Yano et al.[6] reported that several rice mutants with high amylose content (AC) contained starches with B-type XRD patterns. The high-amylose rice mutant Goami 2 (also known as Suweon 464) contained a B-type starch.[7] In maize, high-amylose varieties were also reported to contain B-type starch.[2] However, not all of the high-amylose cereal starches show B-type crystallinity. Some high-amylose rice and barley mutants contain starches with A-type crystallinity.[8,9] Some C-type starches have also been reported in cereals, although only rarely. For example, maize starch with 40% AC was identified as having C-type crystallinity,[2] rice hp-SBE IIb starch showed C-type crystallinity,[10] and starch from the high-amylose rice TRS line also showed C-type crystallinity.[11]

Starch biosynthesis is a complex system comprising four classes of enzymes: ADP-glucose pyrophosphorylase, starch synthase, starch branching enzyme (SBE), and starch debranching enzyme. Each of these enzymes consists of multiple subunits and has several isoforms. Each enzyme plays a distinct role but presumably functions as part of a network. As a part of this complex synthesis pathway, genes controlling amylose synthesis also affect amylopectin formation, and amylopectin can give rise to amylose.[12] Granule-bound starch synthase, encoded by the *Waxy* (*Wx*) gene, is essential for amylose biosynthesis, while amylopectin is synthesized by the combined actions of several isoforms of starch synthase, SBE, and starch debranching enzyme. High-amylose cereals are attracting considerable attention because of their potential health benefits and their wide applications.[10] An increased proportion of amylose in cereals is usually related to increased starch synthase activity or the loss of starch branching enzyme activity.[13] One can overexpress a suitable *Wx* allele, but the more common method is to down-regulate the expressions of genes encoding enzymes involved in amylopectin biosynthesis to direct starch synthesis toward amylose production.[10]

Received: July 12, 2013
Revised: September 12, 2013
Accepted: September 24, 2013
Published: September 24, 2013

dx.doi.org/10.1021/jf4030773 | *J. Agric. Food Chem.* 2013, 61, 9930−9937

The SBEs play a pivotal role in amylopectin biosynthesis by catalyzing chain transfer by cleavage of an α-1,4 linkage following the condensation of an α-1,6 linkage. In cereals such as rice, maize, barley, and wheat, there are three classes of SBEs: SBE I, IIa, and IIb.[14] In rice, SBE I plays a role in the formation of long chains of amylopectin, SBE IIb generates short chains, and SBE IIa partially, but not fully, supports the functions of SBE I and IIb.[15] Cereals have been genetically transformed to increase the AC by blocking amylopectin biosynthesis through mutation or inhibition of the expression of SBE genes.[14] The maize *ae* mutant is deficient in SBE IIb, which resulted in starch with higher AC.[16] In wheat endosperm, suppression of SBE IIa expression resulted in very high AC (>70%).[17] In barley, there was a dramatic increase in AC in endosperm starch when both SBE IIa and IIb were reduced; there was 65.8% AC in the SBE IIa$^-$/IIb↓ line, in which SBE IIa was suppressed with a concomitant reduction in SBE IIb. There was an even higher proportion of AC (89.3%) in the SBE IIa$^-$/IIb$^-$ line, in which both SBE IIa and SBE IIb isoforms were simultaneously suppressed.[18] Amylose-only barley was produced by simultaneously repressing all three SBEs (SBE I, IIa and IIb) by RNA interference.[14] In rice endosperm, the amylose extender mutant IR36*ae* showed increased AC,[13] the inactivation of SBE IIb by RNA silencing increased AC,[10] and simultaneous inhibition of SBE I and IIb by antisense RNA significantly increased AC.[15]

In normal cereal cultivars, the endosperm starch can be waxy, low-, normal-, or high-AC. Cereal mutants and transgenic lines with elevated AC are usually developed from high-AC cereal cultivars, and the structural properties of starches in such lines have been investigated.[13−18] However, there are few reports of mutants and transgenic lines developed from waxy and low-AC cereal cultivars. In general, an increase in AC is accompanied by a change in the crystalline structure of starch from A-type to C- or B-type.[2,6,7,10,11,14,19] The crystalline structure affects the functional properties of starch, especially its thermal properties, digestion, and hydrolysis rates by acid or amylolytic enzymes. A-type starch is more susceptible than C- and B-type starches to digestion and hydrolysis.[11,19−22] It is very important to investigate the crystalline structure of starch for use in food and nonfood industries. However, there is little information on the crystalline structure of starches with elevated AC in mutants and transgenic lines derived from waxy and low-AC cereal cultivars.

Recently, researchers in our laboratory developed several transgenic rice lines with increased AC from three rice cultivars with waxy, low-, and high-AC, by antisense RNA inhibition of both *SBE I* and *IIb*.[15,23] In this study, we isolated starches from mature grains of these transgenic lines and their wild-type parents and investigated the AC and morphology of starches. The crystalline structure of the starches was characterized using XRD, attenuated total reflectance-Fourier transforms infrared (ATR-FTIR), solid-state ^{13}C cross-polarization magic-angle spinning nuclear magnetic resonance (^{13}C CP/MAS NMR), and small-angle X-ray scattering (SAXS) analyses. The objective of this study was to increase our understanding of the role of SBEs in determining the crystalline structure of cereal starches with different ACs.

MATERIALS AND METHODS

Plant Materials. The mature grains of two *japonica* rice cultivars Guang-ling-xiang-nuo (GLXN) and Wu-xiang-9915 (WX), an *indica* rice cultivar Te-qing (TQ), and their transgenic lines were used in this study. The cultivars GLXN, WX, and TQ carry the *wx*, *Wx^b*, and *Wx^a* alleles at the *Wx* locus, which are responsible for waxy, low-, and high-AC in rice endosperm, respectively.[15,24] The 1.3-kb rice glutelin *GluA-3* (*Gt1*) promoter, the 103-bp of intron 2 of rice *Gt1* gene, and the NOS terminator were inserted into the multiple cloning sites of the T-DNA region of the binary vector pCAMBIA1300, which resulted in the intermediate vector p1011. The 680-bp *Xba* I-*Bam*HI fragment at the 5′-end of cloned *SBEI* cDNA and the 997-bp *Sac* I-*Kpn*I fragment at the 5′-end of cloned *SBEIIb* cDNA, at an antisense orientation, were inserted into p1011 between the rice *Gt1* promoter and intron 2 and between the intron 2 and NOS terminator, respectively. Transgenic lines were homozygous for the transgene. Protein blotting analyses showed that both SBE I and IIb proteins were nearly completely inhibited in transgenic lines.[15,23] Rice materials were cultivated in the transgenic close experiment field of Yangzhou University, Yangzhou, China, in the 2010 and 2011 crop years.

Isolation of Starches. Starches were isolated from mature grains according to the method of Wei et al.[25] with some modifications. Brown rice seeds were steeped in distilled water at 4 °C overnight and homogenized with ice-cold water in a home blender. The homogenate was squeezed through five layers of cotton cloth. The residue was homogenized and squeezed twice more in a mortar with a pestle to facilitate the release of starch granules. The combined extract was filtered with 100-, 200-, and 400-mesh sieves and centrifuged at 3000*g* for 10 min. The yellow gel-like layer on top of the packed white starch granule pellet was carefully scraped off and discarded. The process of centrifugation separation was repeated several times until no dirty material existed. The precipitated starch was further washed with anhydrous ethanol two times, dried at 40 °C, ground into powder, and passed through a 100-mesh sieve.

Apparent Amylose Content Measurement. Apparent AC of starches was determined following a modified method[20] according to the iodine adsorption method of Konik-Rose et al.[26] The experiments were performed in triplicate.

Scanning Electron Microscope (SEM) Observation. The starch granules were suspended in anhydrous ethanol. One drop of the starch−ethanol suspension was applied to an aluminum stub using double-sided adhesive tape, and the starch was coated with gold before viewing with an environmental SEM (Philips XL-30).

XRD Analysis. XRD analyses of starches were carried out on an XRD (D8, Bruker, Germany), and the relative crystallinity (%) was measured following the method described by Wei et al.[21] The relative crystallinity was quantitatively determined three times.

ATR-FTIR Analysis. ATR-FTIR analyses of starches were carried out on a Varian 7000 FTIR spectrometer with a DTGS detector equipped with a ATR single-reflectance cell containing a germanium crystal (45° incidence angle) (PIKE Technologies, USA) as previously described.[21] Spectra were corrected by a baseline in the region from 1200 to 800 cm^{-1} before deconvolution was applied using Resolutions Pro. The assumed line shape was Lorentzian with a half-width of 19 cm^{-1} and a resolution enhancement factor of 1.9. The experiments were performed two times.

Solid-State ^{13}C CP/MAS NMR Analysis and Peak-Fitting Procedure. High-resolution solid-state ^{13}C CP/MAS NMR analyses of starches were carried out at *B0* = 9.4T on a Bruker AVANCE III 400 WB spectrometer as described previously.[21] Amorphous starch was prepared by gelatinizing native starch following the method of Wei et al.[21] The ^{13}C CP/MAS NMR spectra were peak fitted by using PeakFit version 4.12. The relative crystallinity was calculated as the proportion of the fitting peak areas of the triplet relative to the total area of the spectrum at the C1 region according to the method described by Paris et al.[27] The quantitative analyses of double-helix, single-helix, and amorphous conformational features within starch were carried out according to the method described by Tan et al.[28] The analyses of the NMR spectra involved the decomposition of the spectra into amorphous and ordered subspectra. The spectrum of amorphous starch was matched to the intensity of native starches at 84 ppm and was subtracted to produce the ordered subspectrum. The areas of the amorphous and ordered subspectra relative to the total area of the spectrum at the C1 region yielded the percentage of amorphous and ordered components, respectively. The computer peak

Table 1. Apparent AC and Relative Crystallinity of Starches in the 2010 and 2011 Crop Years[a]

	apparent amylose content (%)		relative crystallinity (%)[b]	
sample	2010 crop year	2011 crop year	2010 crop year	2011 crop year
GLXN	0.1 ± 0.2 a	0.2 ± 0.3 a	33.5 ± 0.3 a	35.7 ± 0.3 a
GLXN-SBE I/IIb$^-$	6.5 ± 0.4 b	7.2 ± 1.2 b	31.6 ± 0.4 b	32.9 ± 0.2 b
WX	15.2 ± 0.4 c	16.8 ± 1.0 c	29.2 ± 0.3 c	29.6 ± 0.4 c
WX-SBE I/IIb$^-$	23.6 ± 0.6 d	24.6 ± 0.3 d	23.9 ± 0.3 d	24.0 ± 0.7 d
TQ	28.1 ± 0.3 e	26.1 ± 0.2 e	25.9 ± 0.1 e	26.1 ± 0.4 e
TQ-SBE I/IIb$^-$	58.1 ± 0.3 f	57.3 ± 0.5 f	18.5 ± 0.1 f	18.2 ± 1.1 f

[a]Data (mean ± SD) in the same column with different letters were significantly different ($p < 0.05$). [b]Relative crystallinities were obtained from XRD patterns.

fitting of the ordered subspectrum at the C1 region yielded four individual peaks at about 99.5, 100.5, 101.5, and 103 ppm. The peak at 103 ppm was coincident with the C1 chemical shifts of the single-helical V-type conformation, and the peaks at 99.5, 100.5, and 101.5 ppm were double-helix components. By comparison of the areas of single-helix and double-helix peaks at the C1 region in the ordered subspectrum, the relative proportions of single-helical and double-helical features within the starches were obtained.[28] The ^{13}C CP/MAS NMR spectra were quantitatively analyzed three times.

SAXS Analysis. SAXS measurements of starches were performed according to the method of Yuryev et al.[29] with some modifications. Powders of starches were dispersed in an excess of distilled water to form slurries. SAXS measurement was obtained using a Bruker NanoStar SAXS instrument equipped with a Vantec 2000 detector and pinhole collimation for point focus geometry. The X-ray source was a copper rotating anode (0.1 mm filament) operating at 50 kV and 30 W, fitted with cross-coupled Göbel mirrors, resulting in a Cu Kα radiation wavelength of 1.5418 Å. The optics and sample chamber were under vacuum to minimize air scattering. During X-ray exposure, the starch slurries were kept in sealed cells to prevent dehydration. SAXS data sets were analyzed using DIFFRAC^{plus} NanoFit software. The Bragg spacing d was calculated from the position of the peak (q_o) according to $d = 2\pi/q_o$. The experiments were performed two times.

Statistical Analysis. The data reported in all of the tables were mean values and standard deviation. Analysis of variance (ANOVA) by Tukey's test ($p < 0.05$) was evaluated using the SPSS 16.0 Statistical Software Program.

RESULTS AND DISCUSSION

Amylose Contents of Starches. To test the effects of inhibiting *SBE I* and *IIb* on the amylose level, we developed transgenic rice lines from three rice cultivars with different apparent ACs after simultaneous inhibition of both *SBE I* and *IIb* using the antisense RNA technique. Three stable transgenic rice lines with significantly increased ACs were chosen and designated as GLXN-SBE I/IIb$^-$, WX-SBE I/IIb$^-$, and TQ-SBE I/IIb$^-$, according to their wild-type parents (GLXN, WX, and TQ, respectively). In all of these lines, both SBE I and IIb were simultaneously inhibited. Table 1 shows the apparent ACs of starches isolated from mature grains harvested in 2010 and 2011. The apparent ACs of starches in the three transgenic lines were all significantly higher than those of starch in the wild-type parents. Although there were slight differences in the apparent ACs for the same rice material between the two crop years, there was no significant effect of year on apparent AC. Rice varieties can be classified into waxy (0−2%), very low (3−9%)-, low (10−19%)-, intermediate (20−25%)-, or high (>25%)-amylose classes.[30] The results of the present study showed that GLXN, GLXN-SBE I/IIb$^-$, WX, and WX-SBE I/IIb$^-$ were waxy, very low-, low-, and intermediate-amylose varieties, respectively, and that TQ and TQ-SBE I/IIb$^-$ were high-amylose varieties. As determined by the ConA precipitation method, the TQ-SBE I/IIb$^-$ line grains had 55.4% AC, but TQ seeds had only 22.5% AC.[31] The AC estimated from gel permeation chromatography was 44.5% for the TQ-SBE I/IIb$^-$ line but only 20.2% for TQ.[15] The results of gel permeation chromatography indicated that the starch in GLXN-SBE I/IIb$^-$ and WX-SBE I/IIb$^-$ lines had significantly higher ACs than those of the starches in their wild-type parents (data not shown). These results were similar to those reported previously,[10,13] indicating that simultaneous inhibition of SBE I and IIb could dramatically increase the AC of rice grains. The apparent AC increase was more dramatic in TQ-SBE I/IIb$^-$ than in GLXN-SBE I/IIb$^-$ and WX-SBE I/IIb$^-$, probably because TQ is an *indica* rice and has the *Wx*^{a} allele at the *Wx* locus and hence has a more active GBSS I.[13,15]

Morphology of Starch Granules. Figure 1 shows scanning electron microscopy (SEM) images of starch granules isolated from mature grains harvested in 2011. Starch samples from grains harvested in 2010 and 2011 were observed by SEM and were similar in both years (data from 2010 not shown). Starches from three rice cultivars consisted mainly of similar-sized polygonal granules with sharp angles and edges (Figure 1A,C,E). Although the morphologies of starch granules in GLXN-SBE I/IIb$^-$ and WX-SBE I/IIb$^-$ lines were similar to those of starch granules in their wild-type parents, the granules were slightly smaller in the transgenic lines (Figure 1B,D). In terms of morphology and size, the starch granules from the TQ-SBE I/IIb$^-$ line clearly differed from those from the GLXN-SBE I/IIb$^-$ and WX-SBE I/IIb$^-$ lines. Starches from the TQ-SBE I/IIb$^-$ line showed significant heterogeneity. Some starch granules were large, nonangular, and rounded, some were elongated, and some were small and polygonal (Figure 1F). The morphology of starch from the TQ-SBE I/IIb$^-$ line was consistent with that determined in our previous report.[25]

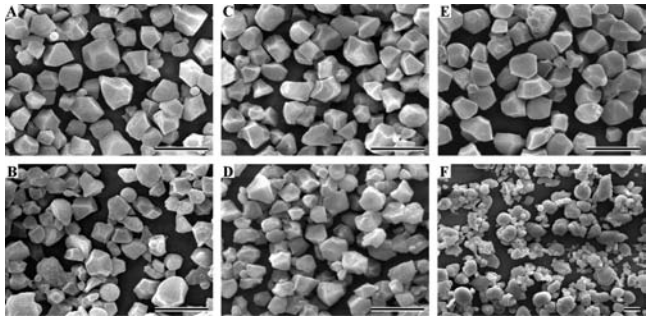

Figure 1. SEM photographs of starch granules in the 2011 crop year. (A) GLXN; (B) GLXN-SBE I/IIb$^-$; (C) WX; (D) WX-SBE I/IIb$^-$; (E) TQ; (F) TQ-SBE I/IIb$^-$. Scale bar = 10 μm.

Starch from the high-amylose rice mutant Goami 2 also showed morphology similar to that of starch from the TQ-SBE I/IIb$^-$ line.[7] Butardo et al.[10] reported that the starch granules isolated from hp-SBE IIb and ami-SBE IIb lines with down-regulated *SBE IIb* were not significantly different from that isolated from their wild-type parent. Elongated starch granules were observed in high-amylose maize *ae* mutants.[19] The different morphologies of starch granules among lines with inhibited SBE I and IIb might be because of the different backgrounds of the wild-type parents. GLXN and WX carry the *wx* and *Wx^b* alleles at the *Wx* locus and are *japonica* rices with waxy and low-ACs. TQ has *Wx^a* allele at the *Wx* locus and is an *indica* rice with high AC.[15,24] Alternatively, differences in the apparent AC among the lines could explain the different morphologies of their starch granules (Table 1).

XRD Spectra of Starches. Starches can be classified into A-, B- and C-type crystallinity based on their XRD spectra. C-type starch is a mixture of both A- and B-type polymorphs and can be further classified to C_A-type (closer to A-type), C-type, and C_B-type (closer to B-type) according to the proportion of A-type and B-type polymorphs.[2] The XRD patterns of starches isolated from mature grains harvested in 2011 are shown in Figure 2. Starch samples from rice grains harvested in 2010

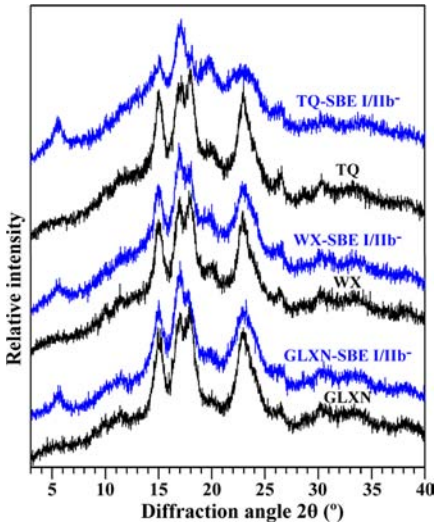

Figure 2. XRD patterns of starches in the 2011 crop year.

showed similar results (data not shown). These XRD patterns were carefully compared with known diffraction patterns of A-, B-, and C-type starches.[2] The starches from three rice cultivars all showed strong reflection at about 15° and 23° 2θ, and an unresolved doublet at 17° and 18° 2θ, which resembled the typical A-type XRD pattern of most ordinary cereal starches.[2] Starches from the GLXN-SBE I/IIb$^-$ and WX-SBE I/IIb$^-$ lines showed strong reflection at about 15°, 17°, and 23° 2θ, a small peak at about 5.6° 2θ, and a shoulder peak at about 18° 2θ. The peak at 5.6° 2θ was characteristic of B-type crystallinity, and the shoulder peak of 18° 2θ° was indicative of the A-type polymorph, which suggested that these starches consisted of A- and B-type polymorphs, with the A-type polymorph being the main component. Therefore, these were C_A-type starches. Starches from the TQ-SBE I/IIb$^-$ line showed strong reflection at about 17° and 5.6° 2θ, a weak reflectant peak at 15° 2θ, and a wide and weak reflectant peak at 23° 2θ. These characters showed that it was a typical C-type starch. The peak at 20° 2θ is indicative of crystalline amylose−lipid complexes.[2] The starch XRD patterns of three rice cultivars showed that WX and TQ starches had amylose−lipid complexes but that GLXN starch did not. The inhibition of both *SBE I* and *IIb* significantly increased the intensity of the peak at 20° 2θ, especially in the TQ-SBE I/IIb$^-$ line, which indicated that more crystalline amylose−lipid complexes were generated (Figure 2).

Cereal starches often show A-type crystallinity, but mutations in SBE IIb often result in starches with B-type crystallinity. Butardo et al.[10] reported that starches in all ami-SBE IIb lines showed full B-type crystallinity. In contrast, some hp-SBE IIb lines retained the A-type starch crystalline polymorph, while others had starch with C-type crystallinity. Tanaka et al.[32] reported that the absence of *SBE IIb* in the mutant EM10 resulted in starch with B-type crystallinity; however, when the mutation was complemented by introducing an *SBE IIb* transgene, the starch crystallinity changed from B-type to A-type via C-type, depending on the strength of transgene expression. Qin et al.[33] reported that starch crystallinity from high-amylose rice changed from A- to C-type via C_A-type during endosperm development. The results of the present study showed that mature rice grains of GLXN-SBE I/IIb$^-$ and WX-SBE I/IIb$^-$ lines contained C_A-type starch, and those of the TQ-SBE I/IIb$^-$ line contained C-type starch. These results indicated that starch with B-type crystallinity accumulated at the middle and/or late stages of endosperm development and that the proportion of the B-type polymorph in starch was lower in the GLXN-SBE I/IIb$^-$ and WX-SBE I/IIb$^-$ lines than in the TQ-SBE I/IIb$^-$ line.

Table 1 shows the relative crystallinities of starches, which were calculated from the XRD patterns. For the three rice cultivars, the crystallinities decreased with the increase in apparent AC. This result was consistent with the findings of Cheetham and Tao,[2] who reported that crystallinity was negatively correlated with AC. The SBE I/IIb$^-$ lines had significantly lower crystallinities than those of their wild-type parents, consistent with the increase in apparent AC resulting from the inhibition of both *SBE I* and *IIb*. There was no significant effect of year on the relative crystallinities of the same rice material.

ATR-FTIR Spectra of Starches. The development of sampling devices like ATR-FTIR combined with procedures for spectrum deconvolution provides opportunities to study starch structure.[34] The infrared spectrum of starch is sensitive to the short-range ordered structure, defined as the double helical order, as opposed to the long-range ordered structure related to the packing of double helices.[35] Although it has been proposed that FTIR is not related to XRD, and it cannot be used to differentiate starches in terms of long-range ordered characteristics and polymorphisms, the variations in spectra among different starches can be interpreted in terms of the short-range ordered structure present in the external region.[34] The intensity of absorbance at 1045, 1022, and 995 cm^{-1} is sensitive to changes in starch conformation. The bands at 1047 (or 1045) and 1022 cm^{-1} are associated with ordered/crystalline and amorphous regions in starch, respectively.[34]

We analyzed starches isolated from mature grains harvested in 2011. The original and deconvoluted ATR-FTIR spectra in the 1200−900 cm^{-1} region are shown in Figure 3. Analyses of starch samples from grains harvested in 2010 showed similar results (data not shown). The spectra of starches from the SBE I/IIb$^-$ lines significantly differed from those of starches from their wild-type parent, especially that of starch from the TQ-

dx.doi.org/10.1021/jf4030773 | J. Agric. Food Chem. 2013, 61, 9930−9937

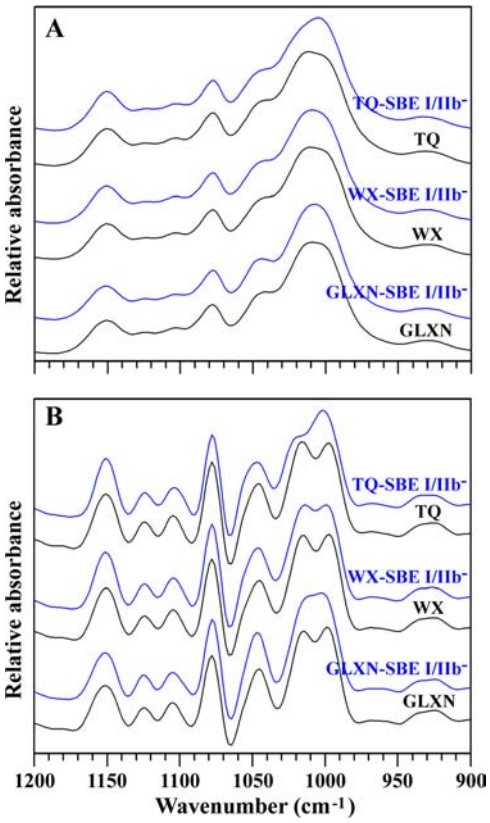

Figure 3. ATR-FTIR spectra of starches in the 2011 crop year. (A) Original spectra; (B) deconvoluted spectra.

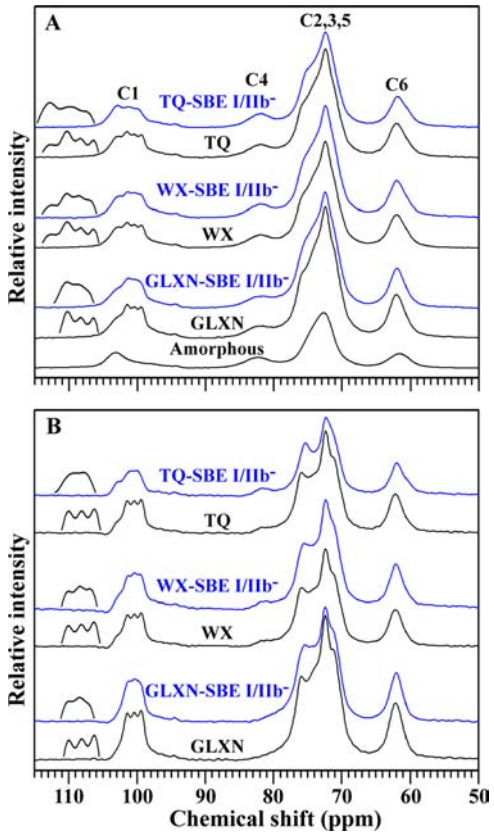

Figure 4. ^{13}C CP/MAS NMR spectra of starches in the 2011 crop year. (A) Original spectra; (B) ordered subspectra.

SBE I/IIb$^-$ line. These results indicated that simultaneous inhibition of both *SBE I* and *IIb* significantly affected the short-range ordered structure in the external region and that the effect was more prominent in the line derived from the high-AC cultivar than in those derived from waxy and low-AC cultivars.

^{13}C CP/MAS NMR Spectra of Starches. The solid-state ^{13}C CP/MAS NMR patterns for starches isolated from mature grains harvested in 2011 are shown in Figure 4. The resonances at different ppm were assigned according to data reported in the literature.[36,37] The C1 resonance, which gives information about both the crystalline nature as well as the noncrystalline (but rigid) chains, has been used to examine the structure of different types of starches. The multiplicity of the C1 resonance corresponds to the packing type of the starch granule. A-type starch, which has three nonidentical sugar residues, shows a triplet at the C1 region, while B-type starch, which has two nonidentical sugar residues, shows a doublet.[38] In general, typical C-type starch has an inconspicuous triplet or doublet at the C1 region. However, C_A-type starch (in which the A-type crystalline structure is predominant) shows a triplet at the C1 region, and C_B-type starch (in which the B-type crystalline structure is predominant) shows a doublet at the C1 region.[36]

The C1 resonances of starches from GLXN, WX, TQ, and the WX-SBE I/IIb$^-$ line occurred as triplets at about 99.5, 100.5, and 101.5 ppm, that of starch from the GLXN-SBE I/IIb$^-$ line showed an inconspicuous triplet, and that of starch from the TQ-SBE I/IIb$^-$ line showed an inconspicuous doublet (Figure 4A). These results, combined with the results from the XRD analysis, further confirmed that the starches from the three rice cultivars were A-type, that from the TQ-SBE I/IIb$^-$ line was C-type, and those from the GLXN-SBE I/IIb$^-$ and WX-SBE I/IIb$^-$ lines were C_A-type, although the C1 resonances of WX-SBE I/IIb$^-$ line starches showed a triplet. The peak at 103 ppm arises from the amorphous domain for C1, and its peak intensity is positively associated with the AC.[28] The peak at 103 ppm was inconspicuous for starches from GLXN and the GLXN-SBE I/IIb$^-$ line appeared only as a shoulder for starches from WX, TQ, and the WX-SBE I/IIb$^-$ line, and was strong for starch from the TQ-SBE I/IIb$^-$ line (Figure 4A). The changes in the intensity of the peak at 103 ppm were consistent with the apparent AC determined by the iodine adsorption method (Table 1).

Figure 4B shows the ordered subspectra of starches. In this analysis, the standard amorphous starch spectrum was subtracted from the test spectrum until there was no residual intensity at 84 ppm (a region of the spectrum with intensity due solely to amorphous conformations).[28] The ordered subspectra were similar to the origin spectra, but they had clearer crystalline peaks of C1 resonances than those in the origin spectra.

The origin and ordered ^{13}C CP/MAS NMR spectra of starches were peak-fitted. A combination (50/50) of Lorentzian and Gaussian profiles gave an acceptable fit (data not shown). The percentage of relative crystallinity and the proportions of single helixes, double helixes, and amorphous components are listed in Table 2. The estimate of crystallinity obtained from ^{13}C CP/MAS NMR was significantly higher than that obtained from XRD analysis. The molecular order in the starch granule reflects two types of helices formed by amylopectin side chains. Helices packed in regular arrays (in the long-range distance) to form crystals can be measured by both XRD and ^{13}C CP/MAS

dx.doi.org/10.1021/jf4030773 | J. Agric. Food Chem. 2013, 61, 9930−9937

Table 2. Relative Crystallinities and Proportions of Single-Helix, Double-Helix, and Amorphous Conformations Obtained from ^{13}C CP/MAS NMR Spectra of Starches in the 2011 Crop Year[a]

sample	relative crystallinity (%)	relative proportion (%)		
		single helix	double helix	amorphous
GLXN	58.9 ± 0.8 a	1.0 ± 0.5 a	61.8 ± 0.5 a	37.2 ± 2.3 a
GLXN-SBE I/IIb$^-$	53.4 ± 0.2 b	1.1 ± 0.6 a	55.5 ± 0.6 b	43.4 ± 2.4 b
WX	51.2 ± 0.4 c	2.4 ± 0.4 b	53.3 ± 0.4 c	44.3 ± 2.6 b
WX-SBE I/IIb$^-$	48.4 ± 1.1 d	3.7 ± 0.5 c	49.4 ± 0.5 d	46.9 ± 2.9 bc
TQ	47.1 ± 1.3 d	3.3 ± 0.4 bc	50.0 ± 0.4 d	46.7 ± 2.6 bc
TQ-SBE I/IIb$^-$	37.2 ± 1.0 e	7.9 ± 0.7 d	39.6 ± 0.7 e	52.5 ± 2.8 c

[a]Data (means ± SD) in the same column with different letters were significantly different ($p < 0.05$).

NMR, whereas those that are not packed in regular form or are packed in the short-range distance can be detected by ^{13}C CP/MAS NMR but not XRD.[38] Therefore, it was not surprising that the estimates of relative crystallinity obtained by ^{13}C CP/MAS NMR were considerably higher than those obtained by XRD analysis. Inhibition of both *SBE I* and *IIb* significantly decreased the relative crystallinity and the amount of double helixes. The decrease was more prominent in the line derived from the high-AC cultivar than in those derived from waxy and low-AC cultivars.

SAXS Spectra of Starches. A comparison of the SAXS patterns of the starches is shown in Figure 5. The well-resolved

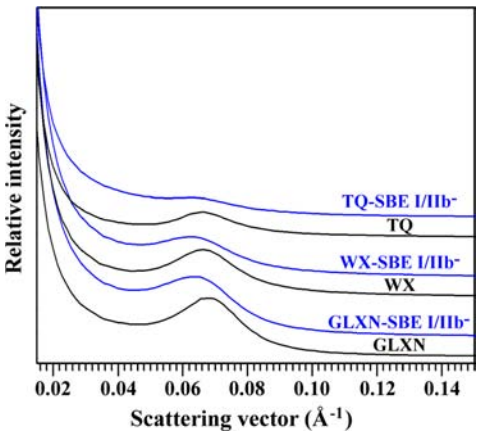

Figure 5. SAXS patterns of starches in the 2011 crop year.

main scattering peak around the scattering vector (q_o) of about 0.06 Å^{-1} is thought to arise from the periodic arrangement of alternating crystalline and amorphous lamellae of amylopectin and corresponds to the lamellar repeat distance or Bragg spacing. The location of the peak depends on the size of lamella and may differ among starches from different plants, while the peak area or intensity depends mainly on the degree of order in semicrystalline regions.[39,40] As shown in Figure 5, all starches were scaled to equal intensity at high q (q = 0.2 Å^{-1}) to account for variations in sample concentrations, according to the method of Sanderson et al.[41] The SAXS patterns were at the same relative scale and, therefore, were directly comparable. GLXN starch showed the most defined lamellar peak centered at 0.067 Å^{-1}, which corresponded to a lamellar repeat distance of 9.37 nm. Starches from WX and TQ showed less defined lamellar peaks, especially TQ starch, but the center of their peaks was the same as that of GLXN starch. Compared with the starch from their wild-type parents, those from SBE I/IIb$^-$ lines showed a reduced lamellar peak intensity, especially that from the TQ-SBE I/IIb$^-$ line, with the peak center shifted toward a lower q_o (0.064 Å^{-1}), corresponding to a longer lamellar repeat distance (9.81 nm). The extremely poorly defined peak for starch from the TQ-SBE I/IIb$^-$ line likely indicated a severely disrupted and/or nonexistent lamellar structure compared to that of starch from its wild-type parent.

Yuryev et al.[29] reported that an increase in AC in native wheat starches was accompanied by decreased peak scattering intensity, which resulted from accumulation of amylose tie-chains with increasing AC in the granules. Compared with the starch from their wild-type parents, the starches from these transgenic rice lines showed significantly lower peak intensities, which might result from the elevated apparent AC. Previously, it was reported that B-type starches have longer average chain-lengths than those of A- and C-type starches, while A-type starches have shorter average chain-lengths than those of C-type starches.[41] The transgenic starches showed C_A- or C-type crystallinity, and the starch from the wild-type parents showed A-type crystallinity (Figures 2 and 4). The SAXS patterns showed that the starches from the transgenic lines had longer Bragg spacing than that of the starches from their wild-type parents, consistent with their crystalline structure. These results showed that simultaneous inhibition of both *SBE I* and *IIb* could increase the lamella size of starch.

In conclusion, the inhibition of both *SBE I* and *IIb* resulted in a significant increase in apparent AC. The increase in apparent AC was more dramatic in the *indica* rice cultivar TQ, which has high-AC starch, than in *japonica* cultivars GLXN and WX, which have waxy and low-AC starches. Inhibition of *SBE I* and *IIb* decreased the size of starch granules in the lines derived from waxy and low-AC rice cultivars, and resulted in the formation of heterogeneous starch granules in lines derived from the high-AC cultivar. The crystalline structure changed from A-type to C_A-type in transgenic rice lines produced from waxy and low-AC cultivars, and to C-type in the transgenic line derived from the high-AC cultivar. Compared with the starches from their wild-type parents, the starches from transgenic rice lines showed significant decreases in relative crystallinity and in the amount of double helixes. The decrease was more prominent in the high-AC cultivar than in the waxy and low-AC cultivars. The inhibition of both *SBE I* and *IIb* significantly affected the short-range ordered structure in the external region, decreased the lamellar peak scattering intensity, and increased the lamella size of starches. The results of this study increased our understanding of the roles of *SBE I* and *IIb* in determining the crystalline structure of cereal starches. This will be useful for exploring the applications of transgenic rice in food and nonfood industries.

dx.doi.org/10.1021/jf4030773 | J. Agric. Food Chem. 2013, 61, 9930−9937

AUTHOR INFORMATION

Corresponding Author

*College of Bioscience and Biotechnology, Yangzhou University, Yangzhou 225009, China. Tel: +86 514 87997217. E-mail: cxwei@yzu.edu.cn.

Funding

This study was financially supported by grants from the Ministry of Science and Technology of China (2012CB944803, 2012AA10A302-7), the National Natural Science Foundation of China (31071342, 31270221), the Funds for Distinguished Young Scientists (BK2012010), and Priority Academic Program Development from Jiangsu Government, China.

Notes

The authors declare no competing financial interest.

ABBREVIATIONS USED

AC, amylose content; ATR-FTIR, attenuated total reflectance-Fourier transform infrared; ^{13}C CP/MAS NMR, ^{13}C cross-polarization magic-angle spinning nuclear magnetic resonance; SBE, starch branching enzyme; SEM, scanning electron microscopy; SAXS, small-angle X-ray scattering; XRD, X-ray powder diffraction

REFERENCES

(1) Gallant, D. J.; Bouchet, B.; Baldwin, P. M. Microscopy of starch: evidence of a new level of granule organization. *Carbohydr. Polym.* **1997**, *32*, 177−191.

(2) Cheetham, N. W. H.; Tao, L. Variation in crystalline type with amylose content in maize starch granules: an X-ray powder diffraction study. *Carbohydr. Polym.* **1998**, *36*, 277−284.

(3) Buléon, A.; Colonna, P.; Planchot, V.; Ball, S. Starch granules: structure and biosynthesis. *Int. J. Biol. Macromol.* **1998**, *23*, 85−112.

(4) Bogracheva, T. Y.; Morris, V. J; Ring, S. G.; Hedley, C. L. The granular structure of C-type pea starch and its role in gelatinization. *Biopolym.* **1998**, *45*, 323−332.

(5) Wang, S. J.; Yu, J. L.; Yu, J. G.; Chen, H. X.; Pang, J. P. The effect of acid hydrolysis on morphological and crystalline properties of Rhizoma *Dioscorea* starch. *Food Hydrocolloids* **2007**, *21*, 1217−1222.

(6) Yano, M.; Okuno, K.; Kawakami, J.; Satoh, H.; Omura, T. High amylose mutants of rice, *Oryza sativa* L. *Theor. Appl. Genet.* **1985**, *69*, 253−257.

(7) Kang, H. J.; Hwang, I. K.; Kim, K. S.; Choi, H. C. Comparative structure and physicochemical properties of IIpumbyeo, a high-quality *japonica* rice, and its mutant, Suweon 464. *J. Agric. Food Chem.* **2003**, *51*, 6598−6603.

(8) Yang, C. Z.; Shu, X. L.; Zhang, L. L.; Wang, X. Y.; Zhao, H. J.; Ma, C. X.; Wu, D. X. Starch properties of mutant rice high in resistant starch. *J. Agric. Food Chem.* **2006**, *54*, 523−528.

(9) Song, Y.; Jane, J. Characterization of barley starches of waxy, normal, and high amylose varieties. *Carbohydr. Polym.* **2000**, *41*, 365−377.

(10) Butardo, V. M.; Fitzgerald, M. A.; Bird, A. R.; Gidley, M. J.; Flanagan, B. M.; Larroque, O.; Resurreccion, A. P.; Laidlaw, H. K. C.; Jobling, S. A.; Morell, M. K.; Rahman, S. Impact of down-regulation of *starch branching enzyme IIb* in rice by artificial microRNA- and hairpin RNA-mediated RNA silencing. *J. Exp. Bot.* **2011**, *62*, 4927−4941.

(11) Wei, C. X.; Xu, B.; Qin, F. L.; Yu, H. G.; Chen, C.; Meng, X. L.; Zhu, L. J.; Wang, Y. P.; Gu, M. H.; Liu, Q. Q. C-type starch from high-amylose rice resistant starch granules modified by antisense RNA inhibition of starch branching enzyme. *J. Agric. Food Chem.* **2010**, *58*, 7383−7388.

(12) Tian, Z. X.; Qian, Q.; Liu, Q. Q.; Yan, M. X.; Liu, X. F.; Yan, C. J.; Liu, G. F.; Gao, Z. Y.; Tang, S. Z.; Zeng, D. L.; Wang, Y. H.; Yu, J. M.; Gu, M. H.; Li, J. Y. Allelic diversities in rice starch biosynthesis lead to a diverse array of rice eating and cooking qualities. *Proc. Natl. Acad. Sci. U.S.A.* **2009**, *106*, 21760−21765.

(13) Butardo, V. M.; Daygon, V. D.; Colgrave, M. L.; Campbell, P .M.; Resurreccion, A.; Cuevas, R. P.; Jobling, S. A.; Tetlow, I.; Rahman, S.; Morell, M.; Fitzgerald, M. Biomolecular analyses of starch and starch granule proteins in the high-amylose rice mutant Goami 2. *J. Agric. Food Chem.* **2012**, *60*, 11576−11585.

(14) Carciofi, M.; Blennow, A.; Jensen, S. L.; Shaik, S. S.; Henriksen, A.; Buléon, A.; Holm, P. B.; Hebelstrup, K. H. Concerted suppression of all starch branching enzyme genes in barley produces amylose-only starch granules. *BMC Plant Biol.* **2012**, *12*, 223.

(15) Zhu, L. J.; Gu, M. H.; Meng, X. L.; Cheung, S. C. K.; Yu, H. X.; Huang, J.; Sun, Y.; Shi, Y. C.; Liu, Q. Q. High-amylose rice improves indices of animal health in normal and diabetic rats. *Plant Biotechnol. J.* **2012**, *10*, 353−362.

(16) Li, L.; Jiang, H. X.; Campbell, M.; Blanco, M.; Jane, J. L. Characterization of maize amylose-extender (*ae*) mutant starches. Part I: relationship between resistant starch contents and molecular structures. *Carbohydr. Polym.* **2008**, *74*, 396−404.

(17) Regina, A.; Bird, A.; Topping, D.; Bowden, S.; Freeman, J.; Barsby, T.; Kosar-Hashemi, B.; Li, Z. Y.; Rahman, S.; Morell, M. High-amylose wheat generated by RNA interference improves indices of large-bowel health in rats. *Proc. Natl. Acad. Sci. U.S.A.* **2006**, *103*, 3546−3551.

(18) Regina, A.; Kosar-Hashemi, B.; Ling, S.; Li, Z. Y.; Rahman, S.; Morell, M. Control of starch branching in barley defined through differential RNAi suppression of starch branching enzyme IIa and IIb. *J. Exp. Bot.* **2010**, *61*, 1469−1482.

(19) Jiang, H. X.; Campbell, M.; Blanco, M.; Jane, J. L. Characterization of maize amylose-extender (*ae*) mutant starches: Part II. structures and properties of starch residues remaining after enzymatic hydrolysis at boiling-water temperature. *Carbohydr. Polym.* **2010**, *80*, 1−12.

(20) Man, J. M.; Yang, Y.; Zhang, C. Q.; Zhou, X. H.; Dong, Y.; Zhang, F. M.; Liu, Q. Q.; Wei, C. X. Structural changes of high-amylose rice starch residues following in vitro and in vivo digestion. *J. Agric. Food Chem.* **2012**, *60*, 9332−9341.

(21) Wei, C. X.; Qin, F. L.; Zhou, W. D.; Yu, H. G.; Xu, B.; Chen, C.; Zhu, L. J.; Wang, Y. P.; Gu, M. H.; Liu, Q. Q. Granule structure and distribution of allomorphs in C-type high-amylose rice starch granule modified by antisense RNA inhibition of starch branching enzyme. *J. Agric. Food Chem.* **2010**, *58*, 11946−11954.

(22) Gérard, C.; Colonna, P.; Buléon, A.; Planchot, V. Amylolysis of maize mutant starches. *J. Sci. Food Agric.* **2001**, *81*, 1281−1287.

(23) Zhang, P. Transgenic-Mediated Knockdown of the Expression of Genes Encoding Starch Branching Enzymes and Its Effects on Grain Quality in Rice (*Oryza sativa* L.). Master's Dissertation. Yangzhou University, Yangzhou, China, 2008.

(24) Sano, Y. Different regulation of waxy gene expression in rice endosperm. *Theor. Appl. Genet.* **1984**, *68*, 4567−4573.

(25) Wei, C. X.; Qin, F. L.; Zhu, L. J.; Zhou, W. D.; Chen, Y. F.; Wang, Y. P.; Gu, M. H.; Liu, Q. Q. Microstructure and ultrastructure of high-amylose rice resistant starch granules modified by antisense RNA inhibition of starch branching enzyme. *J. Agric. Food Chem.* **2010**, *58*, 1224−1232.

(26) Konik-Rose, C.; Thistleton, J.; Chanvrier, H.; Tan, I.; Halley, P.; Gidley, M.; Kosar-Hashemi, B.; Wang, H.; Larroque, O.; Ikea, J.; McMaugh, S.; Regina, A.; Rahman, S.; Morell, M.; Li, Z. Effects of starch synthase IIa gene dosage on grain, protein and starch in endosperm of wheat. *Theor. Appl. Genet.* **2007**, *115*, 1053−1065.

(27) Paris, M.; Bizot, H.; Emery, J.; Buzaré, J. Y.; Buléon, A. Crystallinity and structuring role of water in native and recrystallized starches by ^{13}C CP-MAS NMR spectroscopy 1: spectral decomposition. *Carbohydr. Polym.* **1999**, *39*, 327−339.

(28) Tan, I.; Flanagan, B. M.; Halley, P. J.; Whittaker, A. K.; Gidley, M. J. A method for estimating the nature and relative proportions of amorphous, single, and double-helical components in starch granules by ^{13}C CP/MAS NMR. *Biomacromolecules* **2007**, *8*, 885−891.

(29) Yuryev, V. P.; Krivandin, A. V.; Kiseleva, V. I.; Wasserman, L. A.; Genkina, N. K.; Fornal, J.; Blaszczak, W.; Schiraldi, A. Structural parameters of amylopectin clusters and semi-crystalline growth rings in

wheat starches with different amylose content. *Carbohydr. Res.* **2004**, *339*, 2683−2691.
(30) Kumar, I.; Khush, G. S. Genetic analysis of different amylose levels in rice. *Crop Sci.* **1987**, *27*, 1167−1172.
(31) Zhu, L. J.; Liu, Q. Q.; Wilson, J. D.; Gu, M. H.; Shi, Y. C. Digestibility and physicochemical properties of rice (*Oryza sativa* L.) flours and starches differing in amylose content. *Carbohydr. Polym.* **2011**, *86*, 1751−1759.
(32) Tanaka, N.; Fujita, N.; Nishi, A.; Satoh, H.; Hosaka, Y.; Ugaki, M.; Kawasaki, S.; Nakamura, Y. The structure of starch can be manipulated by changing the expression levels of starch branching enzyme IIb in rice endosperm. *Plant Biotechnol. J.* **2004**, *2*, 507−516.
(33) Qin, F. L.; Man, J. M.; Cai, C. H.; Xu, B.; Gu, M. H.; Zhu, L. J.; Shi, Y. C.; Liu, Q. Q.; Wei, C. X. Physicochemical properties of high-amylose rice starches during kernel development. *Carbohydr. Polym.* **2012**, *88*, 690−698.
(34) Sevenou, O.; Hill, S. E.; Farhat, I. A.; Mitchell, J. R. Organisation of the external region of the starch granule as determined by infrared spectroscopy. *Int. J. Biol. Macromol.* **2002**, *31*, 79−85.
(35) van Soest, J. J. G.; Tournois, H.; de Wit, D.; Vliegenthart, J. F. G. Short-range structure in (partially) crystalline potato starch determined with attenuated total reflectance Fourier-transform IR spectroscopy. *Carbohydr. Res.* **1995**, *279*, 201−214.
(36) Bogracheva, T. Y.; Wang, Y. L.; Hedley, C. L. The effect of water content on the ordered/disordered structures in starches. *Biopolym.* **2001**, *58*, 247−259.
(37) Cheetham, N. W. H.; Tao, L. Solid state NMR studies on the structural and conformational properties of natural maize starches. *Carbohydr. Polym.* **1998**, *36*, 285−292.
(38) Atichokudomchai, N.; Varavinit, S.; Chinachoti, P. A study of ordered structure in acid-modified tapioca starch by ^{13}C CP/MAS solid-state NMR. *Carbohydr. Polym.* **2004**, *58*, 383−389.
(39) Blazek, J.; Gilbert, E. P. Application of small-angle X-ray and neutron scattering techniques to the characterisation of starch structure: a review. *Carbohydr. Polym.* **2011**, *85*, 281−293.
(40) Pikus, S. Small-angle X-ray scattering (SAXS) studies of the structure of starch and starch products. *Fibres Text. East. Eur.* **2005**, *13*, 82−86.
(41) Sanderson, J. S.; Daniels, R. D.; Donald, A. M.; Blennow, A.; Engelsen, S. B. Exploratory SAXS and HPAEC-PAD studies of starches from diverse plant genotypes. *Carbohydr. Polym.* **2006**, *64*, 433−443.